

Return of the cold halocline layer to the Amundsen Basin of the Arctic Ocean: Implications for the sea ice mass balance

G. Björk, J. Söderkvist, and P. Winsor

Department of Oceanography, Earth Sciences Center, Göteborg University, Göteborg, Sweden

A. Nikolopoulos

Department of Meteorology/Physical Oceanography, Stockholm University, Stockholm, Sweden

M. Steele

Polar Science Center, Applied Physics Laboratory, University of Washington, Seattle, USA

Received 1 October 2001; accepted 4 April 2002; published 7 June 2002.

[1] CTD measurements from the Arctic Ocean 2001 expedition reveal that the cold halocline layer (CHL) has returned to the Amundsen Basin at a position close to that found during the Oden'91 expedition. River water from the Siberian shelves formed a strong freshwater front in the Amundsen Basin, extending from the Gakkel Ridge to the Lomonosov Ridge. Furthermore, we show from model computations that the presence of a CHL may increase winter sea ice growth by 0.25 m over one season compared to a case with a non-existing CHL due to increased vertical heat flux from the warm Atlantic water. The difference in sea ice growth is due to a much shallower winter convection with a CHL present, which is not able to reach into the warm Atlantic layer, resulting in a considerably smaller oceanic heat flux. *INDEX TERMS*: 4207 Oceanography: General: Arctic and Antarctic oceanography; 4540 Oceanography: Physical: Ice mechanics and air/sea/ice exchange processes; 4536 Oceanography: Physical: Hydrography; 4255 Oceanography: General: Numerical modeling

1. Introduction

[2] Increasing observational efforts during the last decade have revealed major changes in the Arctic environment, seen in the atmosphere, ice cover and ocean (see *Serreze et al.* [2000] and *Morison et al.* [2000] for recent reviews). One of the major changes observed in the ocean is that the area coverage of the cold halocline layer (CHL) over the Arctic Ocean has decreased substantially. The CHL is characterized by near-constant temperature close to the freezing point while the salinity increases with depth. This characteristic structure covers a large part of the Arctic Ocean in the upper 100 m just below the surface mixed layer (see *Rudels et al.* [1994] and *Steele and Boyd* [1998] for a more detailed description). One important aspect of this layer is that it prevents upward mixing of heat from the Atlantic layer, and thus promotes ice growth during winter. Using data from the Oden'91, SCICEX'93 and SCICEX'95 expeditions *Steele and Boyd* [1998] showed that the halocline layer has

retreated back from the Amundsen Basin into the Makarov Basin comparing the SCICEX'95 data with Oden'91 data, where the data from SCICEX'93 fall somewhere in between. Furthermore, comparing with the *Environmental Working Group (EWG)* [1997] winter data set (1950–1989) they showed that the salinities in the Amundsen Basin during SCICEX'95 were significantly higher than the maximum salinities recorded during the 1950–1989 period.

[3] Here we compare a new icebreaker section of CTD data from summer 2001 and data from the North Pole Experiment Observatory (NPEO), with earlier observations from the same area. The new section, extending from northern Barents Sea to the Makarov Basin, was taken during the Arctic Ocean 2001 expedition by the Swedish icebreaker Oden.

2. Data and Methods

[4] The Arctic Ocean 2001 expedition (AO-01) was a two-month long scientific cruise from 29 June to 28 August mainly in the Barents Sea area surrounding Svalbard and in the Eurasian Basin of the Arctic Ocean. The expedition consisted of several different programs including atmospheric, biogeochemical, seismic, remote sensing, and oceanographic programs. As a part of this expedition (Leg 2 from 17 June to 28 June) a hydrographic section was sampled including 30 stations covering the entire Eurasian Basin from the Barents Sea shelf break across the Lomonosov Ridge and into the Makarov Basin. Vertical profiles of temperature and salinity to at least 1000 m were collected at each station using a CTD instrument. Biogeochemical parameters were also measured and will be reported elsewhere. The CTD used was a Sea Bird 911 plus mounted on a 24-bottle rosette. Pre and post calibrations of the temperature and conductivity sensors together with deep water samples analyzed on a Guildline 8400B Autosol salinometer showed that the CTD had an accuracy of 0.003 and 0.002 in salinity and temperature, respectively. We also use complementary CTD data measured during 2001 from the North Pole Observatory (NPEO'01).

3. Results and Discussion

[5] Figure 1a shows the salinity section along Leg 2 (stations 1–30, for locations see Figure 3d). The salinity in

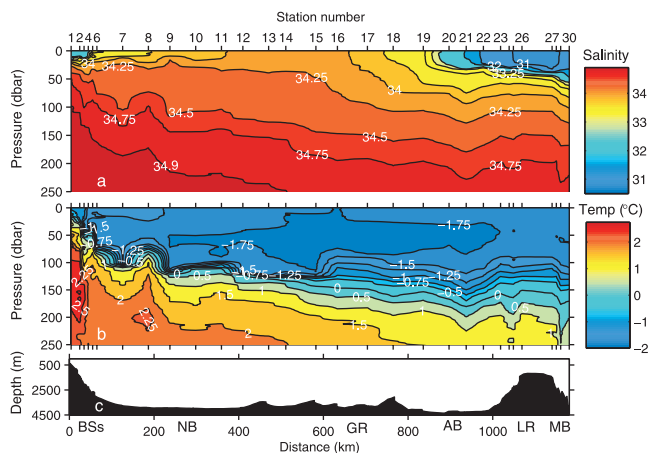


Figure 1. Isopleths of (a) salinity and (b) temperature for stations 1–30 occupied during the AO-01 expedition (for locations see Figure 3d). Figure 1c shows the ocean depth along the transect, from the Barents Sea shelfbreak (BSs) to the Lomonosov Ridge (LR) and into the Makarov Basin (MB). For other abbreviations see Figure 3.

the near surface layer is higher than 34 in the central part of the section represented by stations 11–16. Further north, the salinity decreases abruptly and forms a low salinity surface layer with a minimum salinity less than 31, where the lowest salinities are found in a core confined to the Lomonosov Ridge. The low salinity layer is most likely caused by river input since the freshwater content is much to high in order to be formed by ice melting and it is far away from the inflow of low salinity Pacific water supplied through the Bering Strait. This is supported by previous observations, showing river water domination of the freshwater fraction in this region as diagnosed by $\delta^{18}\text{O}$ tracers [Ekwurzel et al., 2001], and observations of silicate and alkalinity during 1991 [Andersson et al., 1994]. The freshwater content measured as freshwater height integrated down to 100 m and with a reference salinity $S = 34.8$ (see e.g., Björk [1989] for a formal definition) in this layer over the Lomonosov Ridge is typically about 6 m which should be compared to a typical summer ice melt of 0.5 m [Steele and Flato, 2000]. There is also a southern fresher core at the Barents Sea slope (station 1–5) with surface salinity close to 32 at station 3. This core has a maximum freshwater height of 2 m (station 3) and might be a result of extensive ice melting in the northern Barents Sea. A contribution by runoff from Svalbard is also possible. The freshwater height in the central parts of the section is about 1.5 m (see also Figure 2) where the relatively low salinity of about 34.4 in the nearly homogeneous layer between 25 and 120 m is likely a result of initial ice melting from warm Atlantic water in contact with sea ice, which is followed by heat loss, ice growth and relatively deep convection during winter (see Rudels et al. [1996] for a discussion of this mechanism). A summer ice melt signal with salinities in the range 34–34.25 in the upper 25 m is also clearly seen in the central part of the section (see Figure 2, station 12 for an example).

[6] The temperature is near the freezing point in the surface layer over the entire section except at the Barents Sea slope above the warmest core of the inflowing Atlantic

Water (Figure 1b). Station 8 is exceptional with a warmer core and generally thicker layer at high temperature. This is probably the signature of an eddy that has been shed off from the warmer slope current. The eddy is also seen in the density field (not shown here). It is interesting to note that the near-homogeneous surface layer, with temperatures close to the freezing point, is generally deeper in the southern part of the section with depths up to 120 m where the river water influence is absent or very small. The thermocline is also much sharper at stations where the freshwater is absent. We will return later to the issue of how this kind of differences in stratification may affect the ice cover.

[7] Comparing T-S profiles from stations 12 and 22 (Figure 2) shows a well-developed CHL at station 22 but not at station 12 where the salinity stratification is weak all the way down to the sharp thermocline at 120 m.

[8] In order to compare the 2001 observations with earlier expeditions we make use of the same characterization of the cold halocline as in Steele and Boyd [1998] who used the mean salinity in the depth interval 40–60 m as a representative measure of the stratification (and the associated CHL structure). Due to the near-freezing temperatures down to about 100 m depth over most of the section it is possible to identify the CHL by the salinity structure only. The extent of the CHL is then, by definition, the same as the extent of the low salinity layer (below the summer mixed layer). During 1991, a well-developed halocline was present over the entire Amundsen Basin with salinities between 32.3 and 33.6 in the 40–60 m layer, with the lowest values towards Greenland (Figure 3a. The situation was very much different during SCICEX'95 with salinities above 34 across the Amundsen Basin and also relatively high values in the Makarov Basin (Figure 3b). The few existing data points from SCICEX'93 seem to fall in between (see Steele and Boyd [1998]). The extensive hydrographic sections during the ARK XI expedition in 1996 across the Eurasian Basin and Lomonosov Ridge (Schauer et al. [2001]) shows that the halocline is present

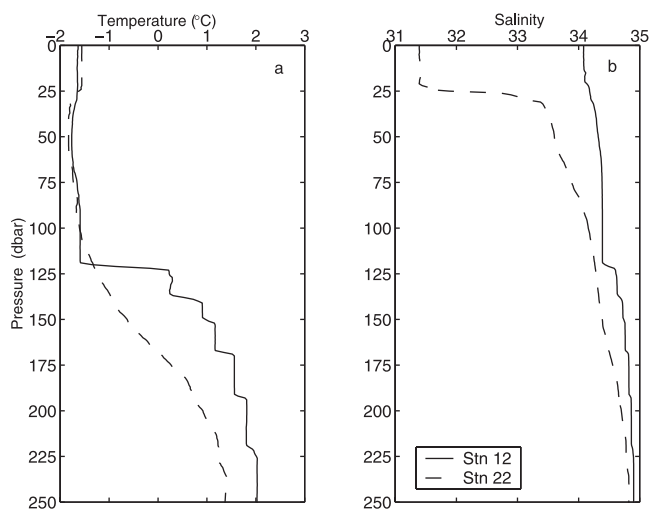


Figure 2. Vertical profiles of (a) temperature and (b) salinity for stations 12 (solid lines) and station 22 (dashed lines). The two profiles represent a typical CHL (station 22) and no CHL (station 12).

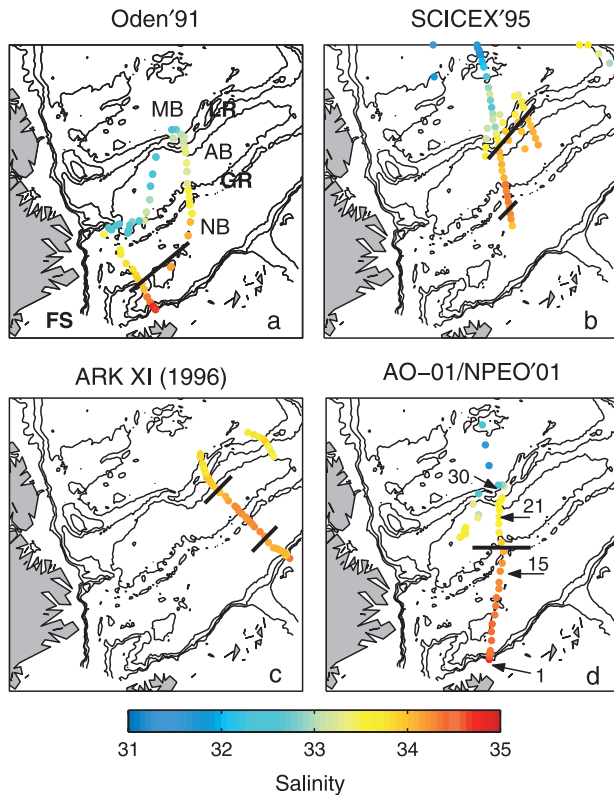


Figure 3. Mean salinity in the interval 40–60 m for (a) Oden'91, (b) SCICEX'95, (c) ARK XI, and (d) AO-01 and NPEO'01. Thick lines show the 34 isohaline. NB = Nansen Basin; AB = Amundsen Basin; MB = Makarov Basin; LR = Lomonosov Ridge; GK = Gakkel Ridge; FS=Fram Strait.

again in the Amundsen Basin (close to the Lomonosov Ridge) but with a much weaker salinity stratification compared to the Oden'91 data (Figure 3c). The 40–60 m salinity is just below 34 in the area from the middle of the Amundsen Basin and further east. Figure 3d shows the new AO-01 section with salinities below 33.75 over the entire Amundsen Basin, closely resembling the Oden'91 situation, but with a slightly weaker salinity stratification. In summary we find that the CHL structure seems to have undergone a back and forth motion over the Amundsen Basin with a retreat back to at least the Lomonosov Ridge in the middle of the 1990s and back again to the Gakkel Ridge in the early 2000s.

[9] Changes in the halocline structure will have consequences for the ice cover since the salinity stratification prevents the convecting surface layer during winter to reach down to the warm Atlantic water. With an absent, or very weak halocline, one can expect a significant reduction of the sea ice growth during winter as a result of upward mixing of heat from the warm layer. In order to quantify the effect of the Arctic halocline on ice growth we have applied a one-dimensional ice-ocean model [Björk, 1997], using an energy-preserving mixed-layer model of a Cato-Phillips type. There is no advection of ice or water in/out of the column. The model is forced by monthly means of air temperature, humidity, downward longwave and shortwave radiation from the North Pole drifting stations [Marshunova and Mishin, 1994], and by wind speed (monthly mean and

standard deviation) from Maykut [1982]. The model was initialized by two sets of vertical profiles of salinity and temperature taken during the AO-01 expedition (see Figure 2), one with a well-developed CHL (station 22), and one without a CHL (station 12). The simulation starts September 1 with an initial ice thickness of 3 m and ice temperature equal to the sea surface temperature.

[10] The main result (Figure 4a) is that the winter sea ice growth is reduced by about 0.25 m for the station with an absent CHL (Station 12) compared with station 22 having a well developed CHL. The winter ice growth is 0.66 m for station 22 and 0.41 m for station 12. The reason for this difference is clearly seen in Figures 4b and 4c showing the mixed layer depth and oceanic heat flux over the simulated time period. A rather complicated time evolution of the ice growth and mixed layer depth is evident in the model. The period starts with an initial phase (September to mid November) when the behavior is quite similar at both stations. This is due to a combination of the initial ice temperature and the presence of a fresher and slightly heated (above the freezing point) surface layer at both stations. Both the near surface layer and the ice has to be cooled before the ice growth can start. The mixed layer becomes much deeper (about 120 m) for station 12 and reach eventually all the way down into the warm Atlantic layer.

[11] The deepening during this period is mostly due to mechanical mixing by the ice motion. The effective mechanical energy supply E is relatively constant and about $1 \times 10^{-4} \text{ W m}^{-2}$ which is used to increase the potential energy of the water column. The entrainment velocity is approximately given by $w_e = 2E/gH\Delta\rho$, where $\Delta\rho$ is the density difference between the mixed layer and the top of the stratified water column, and H is the layer thickness. $\Delta\rho$ is relatively large (0.12 kg m^{-3}) in December since there is a slightly fresher surface layer present, followed by a period with successively decreasing $\Delta\rho$ due to salt supply from sea ice growth giving $\Delta\rho = 0.01 \text{ kg m}^{-3}$ in mid March. $\Delta\rho$ then increases abruptly to 0.1 kg m^{-3} when the mixed layer

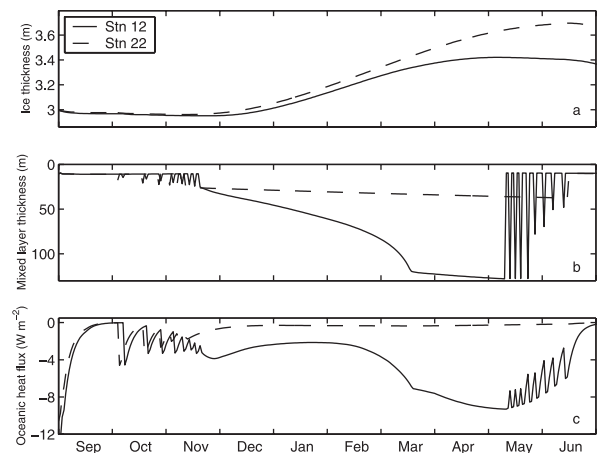


Figure 4. Model simulations of (a) Arctic sea ice thickness, (b) mixed layer thickness, and (c) oceanic heat flux with a CHL (solid line) and no CHL (dashed line). The model was initialized with the profiles shown in Figure 2 and with an initial ice thickness of 3 m.

enters the salinity step at about 125 m depth. The estimated entrainment velocities are 17, 51, and 5 m month⁻¹, using $H = 25, 100,$ and 125 and $\Delta\rho = 0.12, 0.01,$ and $0.1,$ respectively, which explains the basic time development of the mixed layer in Figure 4b. The deep mixing results in a large oceanic heat flux during mid winter and spring. The ice starts to melt in mid April at station 12 compared to mid May for station 22 which also contributes to the total seasonal difference. The water column starts to re-stratify in connection with the onset of ice melt and a shallow mixed layer is established. The maximum heat flux is about 9 W m^{-2} , and occurs just before the re-stratification starts in spring.

[12] The average winter ocean heat flux is 4.5 W m^{-2} in the present computation which is significantly less than the $15\text{--}20 \text{ W m}^{-2}$ in the bulk analysis by *Martinson and Steele* [2001] for an area with comparable weak stratification. One reason for this discrepancy may be that the general time development of the ice-ocean characteristics in our model is very much dependent on the initial ice thickness. Thinner ice gives generally a larger heat flux to the atmosphere, and therefore also larger ice growth which in turn forces stronger convection that deepens the mixed layer faster and increases the oceanic heat flux. The reduction of winter ice growth is 0.84 and 0.5 m (comparing station 12 and 22) for an initial thickness of 1 and 2 m respectively. The average oceanic heat flux is 15 and 9 W m^{-2} for the same initial thicknesses.

[13] The present computation with 3 m initial thickness shows still that the CHL can have a significant effect on the ice growth over a single winter season. A reduction by 0.25 m may also give a significant effect over several years since the ice cover may go from net freezing to net melting. A typical value for the summer ice melt of about 0.5 m (e.g., *Maykut* [1982]) results in a net growth at station 22 over the entire year while station 12 would have a net melt. In order to understand how the CHL will affect the ice cover over several years one has to consider more effects than in this simplified study. Advection will probably play a dominant role in both the water column and ice cover. The ice advection is large in the Amundsen Basin as a result of the transpolar ice drift and the residence time for ice in the area with a fluctuating CHL is relatively short, about 2–3 years. The warm water in the Atlantic layer is also advected through the basin at time scales of 5–15 years [*Ekwurzel et al.*, 2001] which will carry and spread heat, and thereby replenish the heat storage at places with a deep winter mixed layer near the freezing point.

[14] An interesting issue about the CHL is to find the basic control mechanism for the horizontal extent of the structure and also then to find the main cause for such a large difference as between 1995 and 2001. Variations in the wind field has likely an effect and long term changes in the atmospheric pressure pattern between the periods 1979–1987 and 1988–1995 have been shown to correlate with the extent of the river water [*Steele and Boyd*, 1998]. Also a model study by *Johnson and Polyakov* [2001] shows different spreading pattern of river water caused by long term changes in the wind field. The model gives anomalously high salinities in the Laptev Sea and further out in the Eurasian Basin during the period 1994–1996 that corrob-

rates with the observed retreat of the CHL from the Amundsen Basin during 1995. The model salinity anomaly in the upper 50 m is however much weaker (less than 0.4) than the observed changes between 1991 and 1995 that exceeded 1.5.

[15] Our knowledge of the maintenance and spatial variability of the CHL is limited, and merits further investigations to understand how it may affect the Arctic sea ice cover.

[16] **Acknowledgments.** We are grateful to the crew of icebreaker Oden and the Swedish Polar Research Secretariat for the logistic support during the AO-01 cruise. GB was funded by the Swedish Natural Science Research Council (NFR) and the Knut and Alice Wallenberg foundation. MS was funded by NSF OPP-9910305 and OPP-0082770.

References

- Andersson, L. G., G. Björk, O. Holby, E. P. Jones, G. Kattner, K. P. Koltermann, B. Liljeblad, R. Lindegren, B. Rudels, and J. Swift, Water-masses and circulation in the Eurasian Basin: Results from the Oden 91 expedition, *J. Geophys. Res.*, **99**, 3273–3283, 1994.
- Björk, G., A one-dimensional model for the vertical stratification of the upper Arctic Ocean, *J. Phys. Oceanogr.*, **19**, 52–67, 1989.
- Björk, G., The relation between ice deformation oceanic heat flux and the ice thickness distribution in the Arctic Ocean, *J. Geophys. Res.*, **102**, 18,681–18,698, 1997.
- Ekwurzel, B., P. Schlosser, R. A. Mortlock, R. G. Fairbanks, and J. H. Swift, River runoff, sea ice meltwater, and Pacific water distribution and mean residence times in the Arctic Ocean, *J. Geophys. Res.*, **106**, 9075–9092, 2001.
- Environmental Working Group (EWG), Joint U.S.-Russian Atlas of the Arctic ocean [CD-ROM], Nat. Snow and Ice Data Cen., Boulder, Colo., 1997.
- Johnson, M. A., and I. V. Polyakov, The Laptev Sea as a source for recent Arctic Ocean salinity changes, *Geophys. Res. Lett.*, **28**, 2017–2020, 2001.
- Marshunova, M. S., and A. A. Mishin, Handbook of the radiation regime of the Arctic Basin: Results from the drift stations, edited by V. F. Radionov and R. Colony, University of Washington Applied Physics Laboratory Technical Report APL-UW TR9413, 52 pp. plus appendices, 1994.
- Martinson, D. G., and M. Steele, Future of the Arctic sea ice cover: Implications of an Antarctic analog, *Geophys. Res. Lett.*, **28**, 307–310, 2001.
- Maykut, G. A., Large scale heat exchange and ice production in the central Arctic, *J. Geophys. Res.*, **87**, 7971–7984, 1982.
- Morison, J., K. Aagaard, and M. Steele, Recent environmental changes in the Arctic: A review, *Arctic*, **53**, 359–371, 2000.
- Rudels, B., L. G. Anderson, and E. P. Jones, Formation and evolution of the surface mixed layer and halocline of the Arctic Ocean, *J. Geophys. Res.*, **101**, 8807–8821, 1996.
- Schauer, U., B. Rudels, E. P. Jones, L. G. Anderson, R. D. Muench, G. Björk, J. H. Swift, V. Ivanov, and A.-M. Larsson, Confluence and redistribution of Atlantic water in the Nansen, Amundsen and Makarov basins, *Ann. Geophys.*, in press, 2001.
- Serreze, M. C., J. E. Walsh, F. S. Chapin III, T. Osterkamp, M. Dyrugerov, V. Romanovsky, W. C. Oechel, J. Morison, T. Zhang, and R. G. Barry, Observational evidence of recent change in the Northern high-latitude environment, *Clim. Change*, **46**, 159–207, 2000.
- Steele, M., and T. Boyd, Retreat of the cold halocline layer in the Arctic Ocean, *J. Geophys. Res.*, **102**, 10,419–10,435, 1998.
- Steele, M., and G. Flato, Sea ice growth, melt, and modeling: A survey, in *The Freshwater Budget of the Arctic Ocean*, pp 549–587, Kluwer, The Netherlands, 2000.

G. Björk, J. Söderkvist, and P. Winsor, Department of Oceanography, Earth Sciences Center, Göteborg University, 405 30 Göteborg, Göteborg, Sweden. (gobj@oce.gu.se;joso@oce.gu.se;pewi@oce.gu.se)

A. Nikolopoulos, Department of Meteorology/Physical Oceanography, Stockholm University, 106 91 Stockholm, Stockholm, Sweden. (anni@misu.su.se)

M. Steele, Polar Science Center, Applied Physics Laboratory, University of Washington, 1013 NE 40th Street, Seattle, WA 98105-6698, USA.